Journal of Alloys and Compounds 504S (2010) S288–S291

Contents lists available at ScienceDirect

Journal of Alloys and Compounds

journal homepage: www.elsevier.com/locate/jallcom

Composite coating containing WC/12Co cermet and Fe-based metallic glass deposited by high-velocity oxygen fuel spraying

Takeshi Terajima [a,*], Fumiya Takeuchi [a], Kazuhiro Nakata [a], Shinichiro Adachi [b], Koji Nakashima [c], Takanori Igarashi [c]

[a] Joining and Welding Research Institute, Osaka University, 11-1 Mihokaoka, Ibaraki, Osaka 567-0876, Japan
[b] Technology Research Institute of Osaka Prefecture, 2-7-1 Ayumino, Izumi, Osaka 594-1157, Japan
[c] Topy Industries Co., Ltd., 1 Akemicho, Toyohashi, Aichi 441-8074, Japan

ARTICLE INFO

Article history:
Received 4 July 2009
Received in revised form 6 March 2010
Accepted 26 March 2010
Available online 2 April 2010

Keywords:
Metallic glass
Cermet
High-velocity oxygen fuel spraying
Tribological property
Coating materials

ABSTRACT

A composite coating containing WC/12Co cermet and $Fe_{43}Cr_{16}Mo_{16}C_{15}B_{10}$ metallic glass was successfully deposited onto type 304 stainless steel by high-velocity oxygen fuel (HVOF) spraying, and the microstructure and tribological properties were investigated. The microstructure of the coating was characterized by scanning electron microscopy/electron probe micro-analysis (SEM/EPMA) and X-ray diffractometry (XRD). The hardness, adhesion strength and tribological properties of the coating were tested with a Vickers hardness tester, tensile tester and reciprocating wear tester, respectively. The composite coating, in which flattened WC/12Co was embedded in amorphous $Fe_{43}Cr_{16}Mo_{16}C_{15}B_{10}$ layers, exhibited high hardness, good wear resistance and a low friction coefficient compared to the monolithic coating. The addition of 8% WC/12Co to the $Fe_{43}Cr_{16}Mo_{16}C_{15}B_{10}$ matrix increased the cross-sectional hardness from 660 to 870 HV and reduced the friction coefficient from 0.65 to 0.5. WC/12Co reinforcement plays an important role in improving the tribological properties of the $Fe_{43}Cr_{16}Mo_{16}C_{15}B_{10}$ coating.

1. Introduction

Fe-based metallic glass has unique properties in terms of mechanical strength, hardness and corrosion resistance [1–3]. These excellent characteristics originate from atomic disorder and thus are not found in crystalline metals. Therefore, Fe-based metallic glass is a suitable coating material for corrosion and wear protection.

Thermal plasma spraying is a convenient method for applying a thick amorphous coating [4–6]. During the plasma spray process, the starting powder is melted in a plasma torch and then quenched on a substrate. The critical cooling rate required to form an amorphous structure is approximately 10 K/s in the case of Fe-based metallic glass [7]. Thus, it is difficult to produce homogeneous amorphous coating by the liquid-quench process. Furthermore, the plasma spray coating does not afford sufficient protection against corrosion and wear due to defects such as lamellar structures and pores which are unique in plasma spray coating.

Recently, interest has grown in the use of high-velocity oxygen fuel spraying (HVOF) for the application of surface protective coatings [8–9]. A key feature of HVOF is that a high-density coating can be obtained since the starting powder collides with the substrate at a supersonic velocity and is severely deformed. Another key feature is that the process temperature can be controlled to the close range of the glass transition temperatures of metallic glasses as reported in the previous paper [10]. In this paper, the authors discussed the thermal history of Fe based metallic glass powder in the HVOF flame by comparing the coatings deposited by amorphous and crystallized starting powders, respectively. If the powders were heated more than melting temperature in the flame and then were quenched on the substrate, amorphous coatings would be obtained in the each case. However, amorphous coating was actually obtained only from amorphous powder. From these results, it was inferred that Fe based metallic glass powder was heated to the glass transition temperature in the HVOF flame. Around the glass transition temperature, metallic glass transforms into a supercooled state and shows viscous fluidity in spite of temperatures far below its liquidus temperature. Therefore, high-quality metallic glass coatings can be achieved using HVOF spraying.

Recently, studies of Fe-based metallic glass coatings that were applied by the HVOF process have appeared in the literature [11–13]. These reports demonstrated that the Fe-based metallic glass coating remains amorphous after spraying and shows good adhesion to the substrate. However, it was found in the preliminary

* Corresponding author. Tel.: +81 6 6879 4371; fax: +81 6 6879 4371.
E-mail address: terajima@jwri.osaka-u.ac.jp (T. Terajima).

0925-8388/$ – see front matter © 2010 Elsevier B.V. All rights reserved.
doi:10.1016/j.jallcom.2010.03.209

study that the $Fe_{43}Cr_{16}Mo_{16}C_{15}B_{10}$ metallic glass coating exhibited a very low friction coefficient in a lubricating oil environment but a high friction coefficient in a dry environment. Therefore, the monolithic $Fe_{43}Cr_{16}Mo_{16}C_{15}B_{10}$ coating was relatively poor at protecting against wear. One way of improving the tribological properties of $Fe_{43}Cr_{16}Mo_{16}C_{15}B_{10}$ coating is to modify its contact surface. The tribological properties can be considerably influenced by adding second-phase reinforcement such as hard WC/12CO metal. In this study, the production of a WC/12Co–$Fe_{43}Cr_{16}Mo_{16}C_{15}B_{10}$ composite coating via the HVOF process was demonstrated, and the microstructure and tribological properties were investigated.

2. Experimental

$Fe_{43}Cr_{16}Mo_{16}C_{15}B_{10}$ (at%) metallic glass powder was prepared by gas atomization. The particle size was 10–25 μm in diameter. The glass transition temperature T_g and crystallization temperature T_x as measured by differential scanning calorimetry (DSC) at a heating rate of 20 K/min were 875 and 941 K, respectively. The reinforcement used in this study was commercial WC/12Co (Co: 12 wt%) cermet powder having particle sizes of 5–25 μm in diameter. $Fe_{43}Cr_{16}Mo_{16}C_{15}B_{10}$ and WC/12Co powders were homogeneously mixed before spraying. A commercial HVOF spraying system (JP-5000, Praxair Technology Inc., USA), which generates a supersonic flame by combustion of kerosene and oxygen, was used to spray these powders onto a stainless steel substrate. The flow rates of kerosene and oxygen were 0.3 and 850 L/min, respectively. The dimensions of the type 304 stainless steel substrate were 50 mm × 50 mm × 5 mm, and its surface was blasted by a steel grit to improve adhesion. The composite coating was deposited with a thickness of 250–300 μm on the substrate by 16 transverses of the flame gun.

The microstructure of the cross section of the coating was observed by scanning electron microscopy (SEM) and electron probe micro-analysis (EPMA). Crystalline phases of the starting powder and the sprayed coatings were identified by X-Ray diffractometry (XRD) using Cu Kα radiation. The adhesion strength of the coatings was measured using tensile tester. The test specimens were cut into a size of Ø 10 mm × 5 mm and the both coating and substrate surfaces were adhered to jigs with an adhesive (Araldite) to conduct tensile test. The apparent Vickers hardness on the cross section and surface of the coating was measured using a micro Vickers hardness tester at a load of 0.98 N. The measurements were repeated at 20 points on the sample and the results were averaged. The wear properties were measured using a reciprocating wear tester by sliding Ø 4.8 mm Al_2O_3 ball at a load of 1.96 N. The lubricant oil was not used in the wear test. The sliding speed and total sliding time were 20 mm/s and 7200 s, respectively. The abrasion area S of the cross section of the wear track was measured with a stylus surface profiler (Dektak3, Ulvac Co., Ltd.). The specific wear amount W_s was calculated according to the following equation:

$$W_s = \frac{AS}{PL}, \quad (1)$$

where A, P and L are sliding amplitude (5 mm), load (1.96 N) and total sliding distance (144 m), respectively. The friction coefficient was averaged for times from 3600 to 7200 s, a range in which the value of the friction coefficient was stable.

3. Result and discussion

The $Fe_{43}Cr_{16}Mo_{16}C_{15}B_{10}$ powder was successfully prepared by the atomization method. $Fe_{43}Cr_{16}Mo_{16}C_{15}B_{10}$ powder contained mostly spherical particles of Ø 10–25 μm, although some cylindrical particles were also present. WC/12Co powder contained spherical particles of Ø 5–25 μm that were porous. By using starting powders containing 0, 5, 10 and 20 vol% WC/12Co, composite coatings containing 0, 2, 4 and 8 vol% WC/12Co were obtained, respectively. Fig. 1(a) and (b) shows the cross-sectional microstructure of the coatings containing 0% and 8% WC/12Co, respectively. The microstructure exhibited the typical layered structure that is unique to spray coating. EPMA analysis confirmed the dark lamellae to be $Fe_{43}Cr_{16}Mo_{16}C_{15}B_{10}$, while the bright lamellae were identified as WC/12Co. The high-velocity impact of the $Fe_{43}Cr_{16}Mo_{16}C_{15}B_{10}$ powder on the substrate in the supercooling state results in severe plastic deformation and rapid solidification. Therefore, the HVOF spray coating layers were closely adhered to each other. The average porosity fraction in the monolithic $Fe_{43}Cr_{16}Mo_{16}C_{15}B_{10}$ coating was 3%. This decreased to 1% in the coating containing 2% WC/12Co since the WC/12Co splat filled the vacancy between $Fe_{43}Cr_{16}Mo_{16}C_{15}B_{10}$ lamellae. In contrast, the porosity increased to 1.6 and 2.6% in the coating containing 4% and 8% WC/12Co, respectively, due to the vacancies that initially existed inside the WC/12Co powder. Fig. 2 shows XRD patterns of the starting powder containing 10% WC/12Co and the sprayed

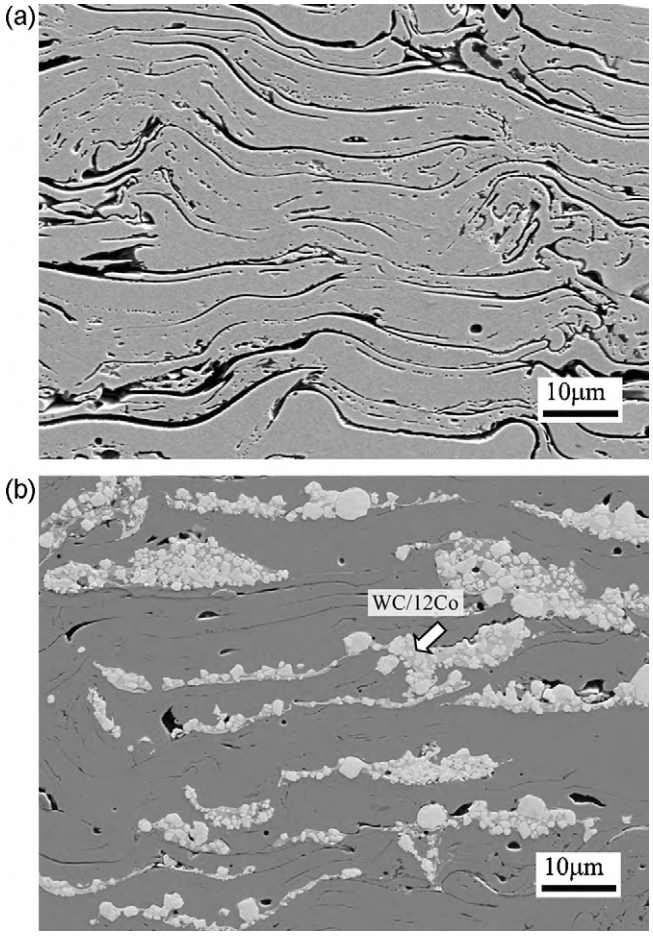

Fig. 1. SEM images of cross section of composite spray coating containing $Fe_{43}Cr_{16}Mo_{16}C_{15}B_{10}$ metallic glass and WC/12Co cermet powders. Volume fractions of WC/12Co were (a) 0% and (b) 8%.

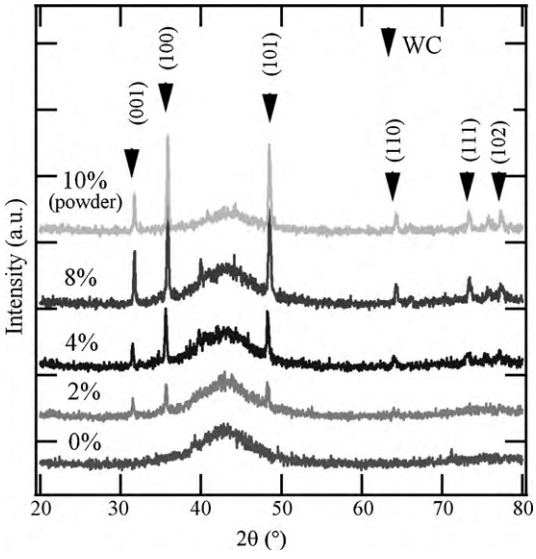

Fig. 2. XRD patterns of WC/12Co–$Fe_{43}Cr_{16}Mo_{16}C_{15}B_{10}$ composite spray coatings and starting powder.

Table 1
Adhesion strength of WC/12Co–$Fe_{43}Cr_{16}Mo_{16}C_{15}B_{10}$ composite spray coatings.

WC/12Co fraction (%)	0	2	4	8	100
Adhesion strength (MPa)	40	41	44	46	47
Fracture position	Coating	Coating	Coating	Adhesive	Adhesive

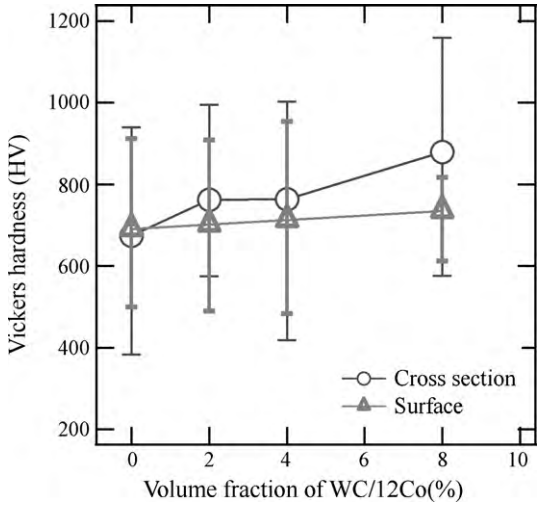

Fig. 3. Vickers hardness (HV) of cross section of WC/12Co–$Fe_{43}Cr_{16}Mo_{16}C_{15}B_{10}$ composite spray coatings.

coatings. Diffraction peaks of WC and the halo pattern between 35° and 50° attributed to amorphous $Fe_{43}Cr_{16}Mo_{16}C_{15}B_{10}$ were observed. These indicate that the atomic disorder of the starting powder was maintained in the sprayed coatings, and no significant decomposition, alloying or oxidation occurred during the spraying process.

Fig. 3 shows the micro Vickers hardness of the surface and the cross section of the coating. The cross-sectional hardness of the monolithic $Fe_{43}Cr_{16}Mo_{16}C_{15}B_{10}$ coating was approximately 660 HV. As the volume fraction of WC/12Co increased, the Vickers hardness gradually increased and reached a value of 870 HV at 8% WC/12Co. In contrast, surface hardness was not considerably affected by the WC/12Co fraction. This anisotropy corresponds to the structure of the coating in which flattened WC/12Co is oriented parallel to the coating surface. The trace of the indentation made by the Vickers test is shown in Fig. 4. This shows that the indenter contacted with not only $Fe_{43}Cr_{16}Mo_{16}C_{15}B_{10}$

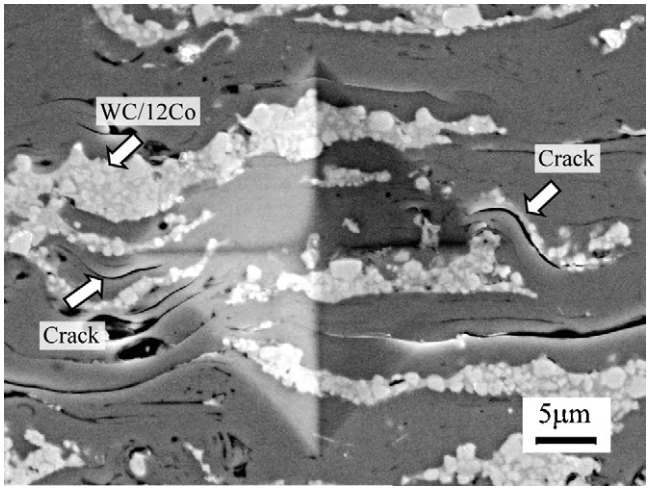

Fig. 4. Trace of indentation in coating containing 8% WC/12Co.

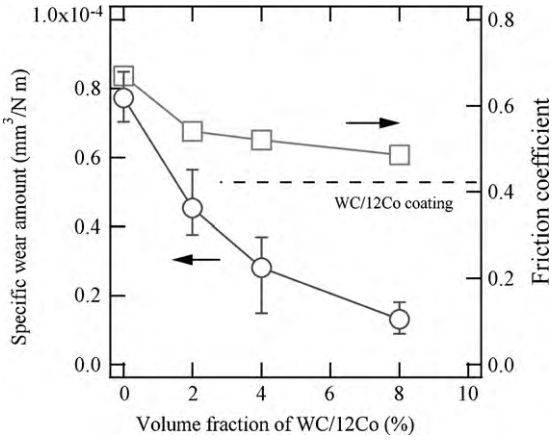

Fig. 5. Abrasion areas and friction coefficients of WC/12Co–$Fe_{43}Cr_{16}Mo_{16}C_{15}B_{10}$ composite coatings.

layers but also hard WC/12Co layers. WC/12Co reinforcement likely helps to increase hardness. However, the Vickers hardness of the sprayed composite coating was even lower than that of bulk material since the coating often cracked along the interfaces

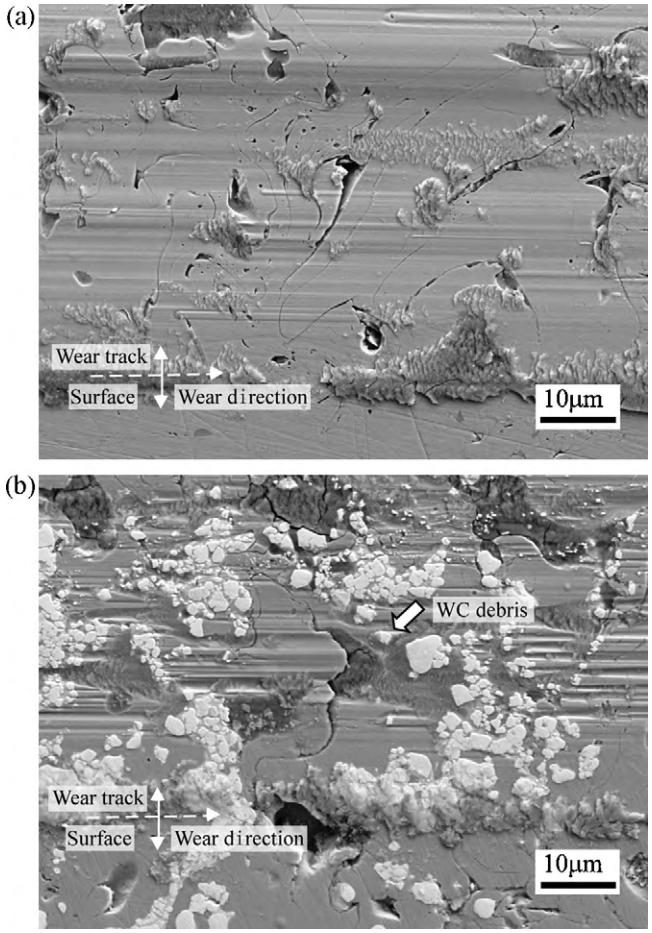

Fig. 6. SEM images of wear tracks of (a) monolithic $Fe_{43}Cr_{16}Mo_{16}C_{15}B_{10}$ coating and (b) composite coating containing 8% WC/12Co.

between the lamellae of the $Fe_{43}Cr_{16}Mo_{16}C_{15}B_{10}$ layers from the corner of the indent where the stress produced by indentation was highest.

Adhesion strength of the coating measured by tensile test was shown in Table 1. The coatings containing 0%, 2% and 4% WC/12Co were fractured in the coatings and their adhesion strength were 40, 41 and 44 MPa, respectively. However, the coatings containing more than 8% of WC/12Co were fractured in the adhesive. Their adhesion strength was estimated at least more than 46 MPa, which was the strength of the adhesive. The adhesion strength of the coating tends to increase slightly with increasing WC/12Co fraction. This tendency corresponds to the behavior of Vickers hardness of the cross section of the coating.

During the initial stage of the reciprocating wear test, the friction coefficient was unstable due to highly adhesive micro-contact between the coating and the Al_2O_3 ball. The friction coefficients were averaged in the range from 3600 to 7200 s and are shown in Fig. 5. It is worth noting that the value of the friction coefficient is not an apparent function of the WC/12Co fraction. However, it did decrease from 0.65 to 0.5, which is close to the value of 0.4 for the monolithic WC/12Co coating as a result of increasing WC/12Co solid lubricant. Furthermore, the presence of 2–8% WC/12Co drastically reduced the specific wear amount from 0.8×10^{-4} to 0.1×10^{-4} $mm^3\,N^{-1}\,m^{-1}$. It is clear that the WC/12Co–$Fe_{43}Cr_{16}Mo_{16}C_{15}B_{10}$ composite coatings have better tribological properties than the monolithic coating.

Fig. 6(a) and (b) shows SEM images of the wear tracks of the monolithic $Fe_{43}Cr_{16}Mo_{16}C_{15}B_{10}$ coating and the composite coating containing 8% WC/12Co, respectively. As shown in Fig. 6(b), the WC/12Co was uniformly distributed and strongly bonded to the $Fe_{43}Cr_{16}Mo_{16}C_{15}B_{10}$ matrix. However, the wear tracks are clearly visible parallel to the sliding direction. This track seems to be formed by scratching with the WC debris peeled from WC/12Co cluster during the wear test since it is not clearly visible for the monolithic $Fe_{43}Cr_{16}Mo_{16}C_{15}B_{10}$ coating as shown in Fig. 6(a). WC/12Co reinforcement plays an important role in the reduction of the friction coefficient and prevention of wear abrasion caused by the Al_2O_3 ball.

4. Conclusions

WC/12Co–$Fe_{43}Cr_{16}Mo_{16}C_{15}B_{10}$ metallic glass composite coating deposited by an HVOF spraying process was demonstrated, and its tribological properties were investigated. The sprayed coatings were successfully coated onto stainless steal without crystallization, decomposition, alloying or oxidation. As the fraction of WC/12Co increased from 0% to 8%, the cross-sectional hardness of the coating increased from 660 to 870 HV; however, surface hardness was little changed. Furthermore, addition of 8% WC/12Co improved the specific wear amount and decreased the friction coefficient from 0.65 to 0.5. It was found that WC/12Co plays important role in improving the tribological properties of the $Fe_{43}Cr_{16}Mo_{16}C_{15}B_{10}$ coating.

Acknowledgement

This work was supported by a Grant-in-Aid for the Cooperative Research Project of Nationwide Joint-Use Research Institutes on the Development Base of Joining Technology for New Metallic Glasses and Inorganic Materials from The Ministry of Education, Culture, Sports, Science and Technology, Japan.

References

[1] S.J. Pang, T. Zhang, K. Asami, A. Inoue, Acta Mater. 50 (2002) 489–497.
[2] M. Iqbal, J.I. Akhter, H.F. Zhang, Z.Q. Hu, J. Non-Cryst. Solids 354 (2008) 3284–3290.
[3] A. Inoue, Acta Mater. 48 (2000) 279–306.
[4] A. Kobayashi, S. Yano, H. Kimura, A. Inoue, Surf. Coat. Technol. 202 (2001) 2513–2518.
[5] K. Kishitake, H. Era, F. Otsubo, J. Therm. Spray Technol. 5 (1996) 476–482.
[6] S. Kumar, J. Kim, H. Kim, C. Lee, J. Alloys Compd. 475 (2009) L9–L12.
[7] J. Shen, Q. Chen, J. Sun, H. Fan, G. Wang, Appl. Phys. Lett. 86 (2005) 151907.
[8] J. Koutsky, J. Mater. Proc. Technol. 557–560 (2004) 557–560.
[9] H.J. Kim, K.M. Lim, G.G. Seong, C.G. Park, J. Mater. Sci. 36 (2001) 49–54.
[10] T. Igarashi, T. Ishikawa, M. Sugiyama, M. Ohara, M. Fukumoto, H. Kimura, A. Inoue, J. Jpn. Therm. Spray. Soc. 45 (2008) 1–4 (in Japanese).
[11] Y. Wu, P. Lin, G. Xie, J. Hu, M. Cao, Mater. Sci. Eng. A 430 (2006) 34–39.
[12] H. Kim, K. Nakata, T. Tsumura, M. Sugiyama, T. Igarashi, M. Fukumoto, H. Kimura, A. Inoue, Mater. Sci. Forum 580 (2008) 467–470.
[13] K. Chokethawai, D.G. McCartney, P.H. Shipway, J. Alloys Compd. 480 (2009) 351–359.